



Strut-and-tie model for FRP effectiveness in shear strengthening of RC deep beams

Tarek S. Mustafa, Fouad B. A. Beshara, Ahmed S. Abd El-Maula & Mustafa G. Fathi

To cite this article: Tarek S. Mustafa, Fouad B. A. Beshara, Ahmed S. Abd El-Maula & Mustafa G. Fathi (2022): Strut-and-tie model for FRP effectiveness in shear strengthening of RC deep beams, European Journal of Environmental and Civil Engineering, DOI: [10.1080/19648189.2022.2056248](https://doi.org/10.1080/19648189.2022.2056248)

To link to this article: <https://doi.org/10.1080/19648189.2022.2056248>



Published online: 04 Apr 2022.



Submit your article to this journal [↗](#)



View related articles [↗](#)



View Crossmark data [↗](#)



Strut-and-tie model for FRP effectiveness in shear strengthening of RC deep beams

Tarek S. Mustafa, Fouad B. A. Beshara, Ahmed S. Abd El-Maula and Mustafa G. Fathi

Civil Engineering Department, Shoubra Faculty of Engineering, Benha University, Cairo City, Egypt

ABSTRACT

In this article, a strut-and-tie model (STM) is proposed for predicting the ultimate shear capacity of fiber reinforced polymers (FRP)-strengthened reinforced concrete deep beams. The proposed STM accounts for the effect of concrete strength, FRP ratio, ratio of main steel, horizontal and vertical stirrups ratio and shear span-to-depth ratio. The ultimate shear predictions of the proposed model are validated with 55 test results from the literature. The comparison showed that the proposed model performs well in predicting the ultimate shear capacity of FRP-strengthened RC deep beams. The overall average value of the ratio between the experimental capacity to the theoretical capacity of the proposed STM ($P_{u(EXP)}/P_{u(STM)}$) is of value 1.16 with a standard deviation of 0.18. Also, comparative studies between the proposed modified STM and the STM provided by the ACI code and other researchers in the literature are presented. Finally, FRP effectiveness studies are performed to study the effect of many structural parameters on the ratio between the ultimate strength for RC deep beams strengthened with FRP materials and the ultimate strength for ordinary RC deep beams. These parameters are FRP ratio (P_{FRP}), the fiber orientation angle to the longitudinal axis of the deep beam, material type of FRP, concrete compressive strength (f'_c) and the shear span-to-depth (a/d) ratio

ARTICLE HISTORY

Received 17 November 2021

Accepted 17 March 2022

KEYWORDS

Reinforced concrete; deep beams; fiber reinforced polymers; strut-and-tie model; ultimate shear capacity

1. Introduction

Deep beams are fairly commonly used as load distribution elements such as transfer girders, pile caps, tank walls, diaphragm beams for folded plates and foundation walls, often receiving many small loads and transferring them to a small number of reaction points. Several definitions are existing for deep beams in the design codes. ACI-318M-14 (ACI Committee 318, 2014) defines the deep beams as members that are loaded on one face and supported on the opposite face such that strut-like compression elements can develop between the loads and supports and to satisfy that the clear span does not exceed four times the overall member depth or concentrated loads exist within a distance of twice the depth from the support face. The strut-and-tie method is a simple method that is considered as an acceptable rational design approach for Disturbed portions (D-regions) of non-flexure members in concrete structure in which, the assumption of simple bending theory do not strictly apply. One such assumption is that in a flexural member such as a beam, plane sections before bending remain plane after bending. A discontinuity of the stress distribution occurs at a change in the geometry of a structural element or at a concentrated load or reaction. The strut-and-tie design method assumes that the load carrying mechanism may be idealized as a hypothetical pin-jointed truss that has inclined compressive struts and longitudinal

tension members called ties inter-connected at truss nodes (Bungale & Taranath, 2012; McCormac & Brown, 2014).

One of the efficient strengthening techniques is the lamination of fiber reinforced polymer (FRP) due to the related superior properties as high tensile strength and stiffness, high resistance to corrosion, excellent fatigue performance and good resistance to chemical attack. FRP lamination is widely accepted by research community and engineering practice in the construction field as a material for strengthening and rehabilitation of major structural defects. Generally, limited analytical researches are found in the literature for the strengthening of RC deep beams with FRP. The outcome of this research outline the way forward and future research focus in this area. FRP, as a strengthening material, has been used to enhance shear capacity of RC beams (Naser et al., 2019). In such application, FRP strengthening systems can be used in variety of techniques including side bonding of FRP sheets and/or plates. Similar to internal steel stirrups, in the case of side bonding of FRP, individual and relatively narrow sheets are bonded and spaced at external sides of the beam to act in parallel for resisting shear forces. An experimental investigation has been carried out (Karayannis & Goliias, 2018) to evaluate the effectiveness of repairing the damaged beam-column connections using FRP sheets after a meticulous but superficial repair of the cracking system using resin paste. Based on the experimental results, it is concluded that the proposed technique can be considered to be a rather satisfactory repair technique for joints with minor to moderate damage considering the rapid, convenient and easy-to-apply character of its application.

Many experimental studies were performed (Al-Ahmed & Al-Jburi, 2016; Al-Ghanem et al., 2017; Asghari et al., 2014; Elsonbaty et al., 2018; Islam et al., 2005; Javed et al., 2016; Khudair & Atea, 2015; Panjehpour et al., 2014; Rasheed, 2016) on the structural response of reinforced concrete deep beams strengthened using CFRP, GFRP and other FRP composite materials. It was found that most of FRP-strengthened RC deep beams show a shear-compression failure due to FRP sheets delamination. Also, all strengthened deep beams give an enhancement in the ultimate load capacity with respect to reference models. An experimental test was carried out (El Maaddawy & Sherif, 2009) to demonstrate the effectiveness of FRP composites on shear strengthening of RC deep beams with openings. It was concluded that the shear strength gain is of range 35–37% due to FRP strengthening. These tests were further examined by FE simulation in a companion study (Hawileh et al., 2012). The results of the numerical study included recommendations to conduct more studies for better understanding of the behaviour of RC beams with openings strengthen with external FRP materials. Other studies were conducted to examine the contribution of FRP flexural reinforcement on the shear strength of RC beams (Hawileh et al., 2015; Nawaz et al., 2016). Strengthened beams showed a 13% to 138% increase in shear capacity due to installing thin FRP sheets along the soffit of the beams (Nawaz et al., 2016). However, the technology for structure strengthening with FRP strips still needs to be improved. Some problems arise from the fact that FRP strips exhibit insignificant strength in direction perpendicular to the fibers, and practically do not carry any bending moments, hence even small imperfections can lead to premature failure of the strip. The issues of fire protection or exposure to harmful environments are also often difficult to solve and needs some evaluation. To prevent de-bonding of FRP sheets from concrete surface, and to prevent delamination of concrete cover with FRP layers, surface preparation and perfect epoxy-based bonding with existing substrate are extremely important.

The aim of this article is to present an analysis and design tool using strut-and-tie model (STM) for reinforced concrete deep beams strengthened with FRP materials (Fathi, 2021). The proposed STM accounts for the contribution of FRP strengthening materials in order to predict the ultimate shear capacity for RC deep beams strengthened with FRP materials. In addition, validation studies for the proposed STM are made for 55 tested deep beams from other experimental researchers in the literature (Al-Ahmed & Al-Jburi, 2016; Al-Ghanem et al., 2017; Asghari et al., 2014; Elsonbaty et al., 2018; Islam et al., 2005; Javed et al., 2016; Khudair & Atea, 2015; Panjehpour et al., 2014; Rasheed, 2016). Comparative studies between the proposed STM, the ACI code (ACI Committee 440, 2008) and the Triantafillou and Antonopoulos model (Triantafillou & Antonopoulos, 2000) are presented. Finally, FRP effectiveness studies are performed to study the effect of parameters of FRP strengthening materials such as FRP ratio (ρ_{FRP}), the fiber orientation angle to the longitudinal axis of the deep beam and the material type of FRP, the effect of concrete compressive strength (f'_c) and the effect of the shear span-to-depth (a/d) ratio on the ratio between the ultimate strength for RC deep beams strengthened with FRP materials and the ultimate strength for ordinary RC deep beams.

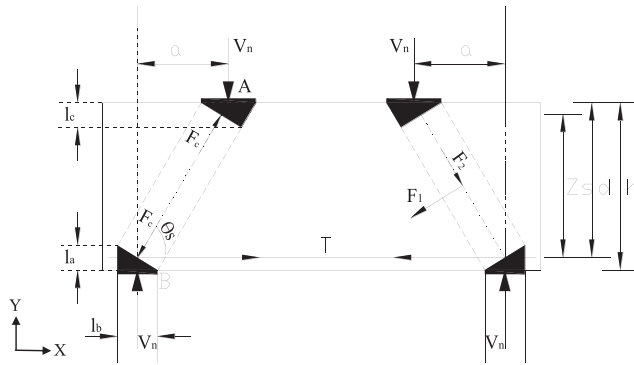


Figure 1. Strut-and-tie model for simply supported deep beam (correct notations).

2. Mathematical formulation of the proposed STM

2.1. Main assumptions and limitations

In Hanoon et al. (Hanoon, Jaafar, Al Zaidee, et al., 2017; Hanoon, Jaafar, Hejazi, et al., 2017), a sophisticated STM model was proposed to predict the shear strength of CFRP-strengthened RC deep beams only. It utilizes a particle swarm optimization algorithm, in which the optimal STM of CFRP-strengthened deep beams is determined by searching for the optimum unknown coefficients. Also, the numerical results of 325 simulated finite element models for deep beams, are used to derive the unknown coefficients. In this article, the proposed model is a simpler version of the model of (Hanoon, Jaafar, Al Zaidee, et al., 2017). It adopts the traditional trail-and-error technique for obtaining the unknown coefficients of the proposed model on the basis of failure modes and geometry constraints. It is derived in a general form for RC deep beams; strengthened with any FRP material such as CFRP, GFRP and AFRP. To modify the applicability of the STM for RC deep beams strengthened with FRP composite materials, the following limitations and assumptions are considered (Fathi, 2021):

1. The proposed STM is applied for simply supported reinforced concrete deep beams; strengthened with FRP materials;
2. Uniaxial compressive stress is created through the concrete strut that inclined at an angle θ with the longitudinal axis of the deep beam;
3. Perfect bond is assumed between the concrete surface and the FRP materials that treated as conventional shear reinforcement in terms of forces distribution for continuously bonded sheet or discontinuously bonded vertical strips;
4. The proposed STM considers the tensile rupture failure mode of FRP composite materials, concrete crushing and diagonal splitting concrete failure mode.

The current version of the proposed model assumes that no delamination or de-bonding of FRP strengthening layers are allowed. In future studies, such local failure phenomena can be included in similar way to what proposed in (Hanoon, Jaafar, Hejazi, et al., 2017).

2.2. Shear resistance mechanisms in deep beams

Figure 1 represents the geometrical properties of the proposed STM for the deep beam (Fathi, 2021). As shown in the figure, two stresses are created through the diagonal concrete strut due to the applied load. The first stress is a compressive stress (f_2) that formed through a direction connected between the applied load and the support. The formation of a concrete crushing failure in the strut caused by the first compressive stress and should be resisted by the concrete compressive strength (CEB-FIP, 1993; CSA-A23.3, 1994). The second stress is a transverse tensile stress (f_1) that applied in a direction perpendicular to the concrete strut. This stress causes the possible concrete splitting failure that can be resisted by the longitudinal and transverse reinforcement, concrete tensile strength and FRP materials.

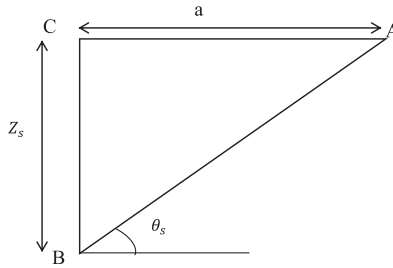


Figure 2. Illustrative sketch for the inclination angle between the compressive strut and the tension tie.

Applying the equilibrium equations at the bottom nodal zone (B) of the diagonal concrete strut which experiences a biaxial tension-compression stress state as shown in [Figure 1](#):

$$\sum F_y = 0; F_c = \frac{V_n}{\sin\theta_s} \quad (1)$$

$$\sum F_x = 0; T = \frac{V_n}{\tan\theta_s} \quad (2)$$

The angle of inclination (θ_s) of the inclined strut as shown in [Figure 2](#) can be defined as:

$$\theta_s = \tan^{-1}\left(\frac{Z_s}{a}\right) \quad (3)$$

where

(F_c) = the compressive force applied through the inclined strut;

(T) = the tensile force applied through the horizontal tie;

(V_n) = the applied load;

(a) = the shear span measured from the applied load to the support;

(Z_s) = the lever arm connected between the longitudinal reinforcement and the center of the upper node of the diagonal strut (Tang & Tan, 2004) and can be defined as;

$$Z_s = h - \frac{l_a}{2} - \frac{l_c}{2} \quad (4)$$

where

(h) = the overall depth of the deep beam;

(l_a) = the depth of the bottom nodal zone of the inclined strut;

(l_c) = the depth of the top nodal zone of the inclined strut;

The compressive stress applied to the inclined concrete strut (f_2) can be calculated from [Equation \(1\)](#):

$$f_2 = \frac{F_c}{A_{str}} = \frac{V_n}{A_{str} \sin\theta_s} \quad (5)$$

where (A_{str}) is the cross- sectional area of the diagonal strut and can be calculated by the following:

$$A_{str} = b_w * (l_a \cos\theta_s + l_b \sin\theta_s) \quad (6)$$

where

(b_w) = the width of the deep beam;

(l_b) = the width of the support-bearing plate;

To calculate the principal tensile stress (f_1) perpendicular to the inclined concrete strut at the bottom nodal zone, a deep beam should be considered (Tong, 1997):

$$f_1 = \frac{KT \sin\theta_s}{A_c / \sin\theta_s} \quad (7)$$

where (A_c) is the cross- sectional area of the deep beam and can be calculated by the following:

$$A_c = b_w * h \quad (8)$$

The term $(T \sin \theta_s)$ is considered to present the component of (T) in the principal tensile direction of the bottom nodal zone. The stress distribution along the diagonal strut is nonlinear and cannot be calculated directly by beam theory assumptions. Therefore, more studies are required to determine stress distribution factors (K_1 and K_2) which refer to the stress distribution factors at the bottom and top nodal zones, respectively.

Based on the forces equilibrium, previous studies (Tan et al., 2001; Zeng & Tan, 1999) determined the values of stress distribution factors as $K_1 = 2$ and $K_2 = 0$ which indicates a good agreement with the experimental results for reinforced concrete deep beams.

2.3. The concrete strut softening effect

Linear interactive failure criteria, such as the modified Mohr–Coulomb theory, is utilized to account for the concrete softening effect under biaxial tension-compression stress state in the bottom nodal zone of the inclined strut. This theory takes into consideration that the critical shear stress is related to the internal friction (Ugural & Fenster, 2003) and uses the following equation:

$$\frac{f_1}{f_t} + \frac{f_2}{f_c'} = 1 \quad (9)$$

where

f_t = tensile strength contribution of concrete, reinforcement and FRP materials and it displays the maximum tensile capacity in the (f_t) tensile direction;

f_c' = cylinder compressive strength of concrete and it represents the maximum compressive capacity in the (f_2) compressive direction;

The term (f_t) presents the combined tensile strength contribution of longitudinal reinforcement, vertical, horizontal web reinforcement, FRP composite materials and concrete and can be calculated by:

$$f_t = f_{t1} + f_{t2} + f_{t3} + f_{t4} \quad (10)$$

$$f_{t1} = \frac{K A_s f_y \sin \theta_s}{A_c / \sin \theta_s} \quad (11)$$

where

A_s = the total area of the longitudinal steel reinforcement;

f_y = the yield strength of the longitudinal steel reinforcement;

The Equation (11) represents the tensile strength contribution of the longitudinal steel reinforcement and is derived by the similar fashion as the term (f_{t1}) in Equation (7).

$$f_{t2} = \frac{2 A_w f_{yw} \sin(\theta_s + \theta_w)}{A_c / \sin \theta_s} \quad (12)$$

where

A_w = the total area of the web steel reinforcement;

f_{yw} = the yield strength of the web steel reinforcement;

The Equation (12) displays the tensile capacity contribution of the inclined web reinforcement at an angle (θ_w) with the longitudinal axis of the deep beam. It takes into consideration the different arrangements of the web steel reinforcement, be it vertical, horizontal, inclined or combined. Therefore, it can be written as the following:

$$f_{t2} = \frac{2 A_{sv} f_{yv} \sin(\theta_s + \theta_{vv})}{A_c / \sin \theta_s} + \frac{2 A_{sh} f_{yh} \sin(\theta_s + \theta_{wh})}{A_c / \sin \theta_s} \quad (13)$$

where

A_{sv} = the total area of the vertical web steel reinforcement within the distance of the shear span;

f_{yv} = the yield strength of the vertical web steel reinforcement;

A_{sh} = the total area of the horizontal web steel reinforcement within the distance of the shear span;

f_{yh} = the yield strength of the horizontal web steel reinforcement;

For simplicity, if the value of (θ_{wv}) equals to (90 degree) for the vertical web steel reinforcement and the value of (θ_{wh}) equals to (zero) for the horizontal web steel reinforcement. Therefore, the Equation (13) can be reduced to the following:

$$f_{t2} = \frac{2A_{sv}f_{yv}\text{Sin}(2\theta_s)}{2A_c} + \frac{2A_{sh}f_{yh}\text{Sin}^2(\theta_s)}{A_c} \quad (14)$$

The third term is the tensile strength contribution of the FRP composite materials and can be expressed by the following equation:

$$f_{t3} = \frac{2n_f A_{FRP} f_{f,FRP} \text{Sin}(\theta_s + \theta_{w,FRP})}{A_c / \text{Sin}\theta_s} \quad (15)$$

where

n_f = the number of the FRP material layers;

A_{FRP} = the total area of the FRP material;

$f_{f,FRP}$ = the ultimate strength of the FRP material;

$\theta_{w,FRP}$ = the orientation angle of the FRP material with respect to the longitudinal axis of the deep beam;

Finally, the last contribution is the tensile strength contribution from concrete which is given by Tan et al. (2001) as follows:

$$f_{t4} = f_{ct} = 0.5\sqrt{f'_c} \quad (16)$$

2.4. Derivation of strut effectiveness factor

Many theoretical models (Foster, 1992; Tanapornraweekit et al., 2011; Vecchio & Collins, 1986) have been suggested to consider the effect of compression softening on concrete strength due to cracking under tension-compression stress states. Based on the proposed STM, the expression that yields the diagonal concrete strut effectiveness factor (μ) can be written as follows:

The compressive stress (f_2) along the inclined strut should not exceed the cylinder compressive strength of concrete (f'_c):

$$f_2 \leq f'_c \quad (17)$$

Substituting Equation (5) into Equation (17), the following expression can be obtained:

$$\frac{F_c}{A_{str}} = \mu f'_c \quad (18)$$

Substituting Equations (5), (7) and (18) into Equation (9), the following expression can be obtained:

$$\mu = 1 - \frac{KT\text{Sin}^2\theta_s}{A_c f_t} \quad (19)$$

where the component (T) refers to the tension force applied through the horizontal tie as displayed in Figure 1 and equals to the tensile force in the bottom steel reinforcement. Therefore, the following equation for the effectiveness factor is created:

$$\mu = 1 - \frac{A_s f_y \text{Sin}^2\theta_s}{A_c f_t} \quad (20)$$

Finally, the nominal shear capacity (V_n) can be obtained by substituting Equation (5) into Equation (18) as follows:

$$V_n = \mu A_{str} f'_c \text{Sin}\theta_s \quad (21)$$

The value of the inclination angle (θ_s) of the inclined strut with respect to the longitudinal axis of the deep beam is influenced by the bottom tie depth (l_a) and the depth of the top node (l_c) which can be obtained as follows:

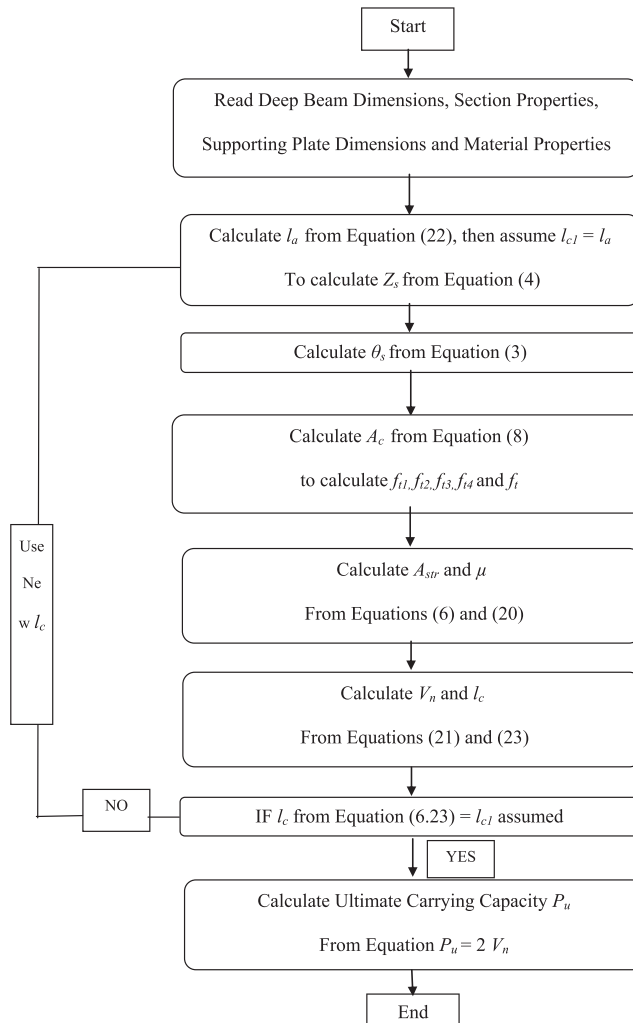


Figure 3. Implementation flow chart for the ultimate strength of FRP-strengthened RC deep beams.

$$l_a = 2*(h - d) \quad (22)$$

where

(h) = the overall depth of the deep beam;

(d) = the effective depth of the deep beam;

The depth of the top node (l_c) can be calculated by the equilibrium limit of the top node and can be determined from the following equation if a stress limit of $(0.85 f'_c)$ is imposed on the top node:

$$l_c = \frac{V_n}{0.85 f'_c b_w \tan \theta_s} \quad (23)$$

The value of (l_c) cannot be determined at first. Consequently, the inclination angle (θ_s) cannot be calculated, which makes an iterative method necessary. The value of the nominal shear capacity (V_n) can then be determined by utilizing Equation (21) during the iterations.

3. Model implementation and validation studies

Figure 3 shows the steps of iteration to determine the ultimate capacity of reinforced concrete deep beams strengthened with FRP composite materials.

Table 1. STM predictions of ultimate load capacity.

No.	Ref.	f_c' (MPa)	b_w (mm)	h (mm)	L (mm)	a/d	ρ_s (%)	ρ_v (%)	ρ_h (%)	ρ_{FRP} (%)	f_{FRP} (MPa)	P_{FRP} (kN)	P_{USTM} (kN)	P_{USTM} (kN)	P_{JSTM} (kN)	P_{JSTM} (kN)	P_{ACI} (ACI Committee 440, 2008)	P_{ACI} (ACI Committee 440, 2008)	P_{Ultra} (Triantafyllou & Antonopoulos, 2000)
1	(Panjehpour et al., 2014)	37.02	140	350	1840	0.75	4.48	0.404	0.404	0.157	3900.00	905.30	799.70	1.24	1.59	1.59	1.59	1.59	1.86
2	(Panjehpour et al., 2014)	37.02	140	350	1840	1.00	4.48	0.404	0.404	0.157	3900.00	857.90	767.22	1.21	1.51	1.51	1.51	1.51	1.64
3	(Panjehpour et al., 2014)	37.02	140	350	1840	1.25	4.48	0.404	0.404	0.157	3900.00	740.00	701.00	1.15	1.30	1.30	1.30	1.30	1.34
4	(Panjehpour et al., 2014)	37.02	140	350	1840	1.50	4.48	0.404	0.404	0.157	3900.00	691.10	629.60	1.20	1.21	1.21	1.21	1.21	1.19
5	(Panjehpour et al., 2014)	37.02	140	350	1840	1.75	4.48	0.404	0.404	0.157	3900.00	510.00	564.237	0.99	0.90	0.90	0.90	0.90	0.85
6	(Panjehpour et al., 2014)	37.02	140	350	1840	2.00	4.48	0.404	0.404	0.157	3900.00	468.10	507.63	1.01	0.82	0.82	0.82	0.82	0.76
7	(Hanoon et al., 2017)	41.60	102	280	1400	1.00	3.30	-	-	0.325	3800.00	325.00	293.00	1.21	1.39	1.39	1.39	1.39	2.81
8	(Hanoon et al., 2017)	41.60	102	280	1400	1.00	3.30	-	-	0.163	3800.00	276.00	272.00	1.11	1.77	1.77	1.77	1.77	1.87
9	(Hanoon et al., 2017)	41.60	102	280	1400	1.00	3.30	-	-	0.163	3800.00	291.00	287.00	1.11	1.55	1.55	1.55	1.55	1.66
10	(Hanoon et al., 2017)	41.60	102	280	1400	1.00	3.30	0.37	-	0.325	3800.00	343.00	298.00	1.26	1.16	1.16	1.16	1.16	1.92
11	(Hanoon et al., 2017)	41.60	102	280	1400	1.00	3.30	0.37	-	0.163	3800.00	320.00	280.00	1.25	1.46	1.46	1.46	1.46	1.52
12	(Hanoon et al., 2017)	41.60	102	280	1400	1.00	3.30	0.37	-	0.163	3800.00	335.00	293.00	1.25	1.34	1.34	1.34	1.34	1.40
13	(Hanoon et al., 2017)	41.60	102	280	1400	1.75	3.30	0.37	-	0.325	3800.00	255.00	260.00	1.07	0.86	0.86	0.86	0.86	1.00
14	(Hanoon et al., 2017)	41.60	102	280	1400	1.75	3.30	0.37	-	0.163	3800.00	290.00	248.00	1.28	1.33	1.33	1.33	1.33	1.11
15	(Hanoon et al., 2017)	41.60	102	280	1400	1.75	3.30	0.37	-	0.163	3800.00	278.00	249.00	1.22	1.11	1.11	1.11	1.11	0.89
16	(Al-Ghanem et al., 2017)	30.00	190	400	1900	1.19	1.87	-	-	0.179	4900.00	653.00	612.00	1.17	1.60	1.60	1.60	1.60	1.85
17	(Al-Ghanem et al., 2017)	30.00	190	400	1900	1.19	1.87	-	-	0.631	3000.00	410.00	541.00	0.83	0.99	0.99	0.99	0.99	2.04
18	(Al-Ghanem et al., 2017)	30.00	190	400	1900	1.19	1.87	-	-	0.631	3000.00	507.00	580.00	0.96	0.98	0.98	0.98	0.98	2.32
19	(Rasheed, 2016)	34.00	115	400	1200	1.00	1.50	-	-	0.075	3500.00	418.00	372.09	1.23	2.51	2.51	2.51	2.51	2.23
20	(Rasheed, 2016)	34.00	115	400	1200	1.00	1.50	0.109	0.257	0.075	3500.00	535.00	382.89	1.53	1.85	1.85	1.85	1.85	1.72
21	(Rasheed, 2016)	34.00	115	400	1200	1.00	1.50	0.307	0.447	0.075	3500.00	469.00	390.59	1.31	1.12	1.12	1.12	1.12	1.06
22	(Rasheed, 2016)	34.00	115	400	1200	1.00	1.50	0.364	-	0.075	3500.00	555.00	386.19	1.57	1.92	1.92	1.92	1.92	1.79
23	(Rasheed, 2016)	34.00	115	400	1200	1.00	1.50	0.615	-	0.075	3500.00	604.00	392.09	1.69	1.62	1.62	1.62	1.62	1.53
24	(Rasheed, 2016)	34.00	115	400	1200	1.00	1.50	-	0.486	0.075	3500.00	518.00	383.95	1.48	1.57	1.57	1.57	1.57	1.48
25	(Rasheed, 2016)	34.00	115	400	1200	1.00	1.50	-	0.757	0.075	3500.00	472.00	389.05	1.33	1.12	1.12	1.12	1.12	1.07
26	(Rasheed, 2016)	34.00	115	500	1200	0.80	1.17	0.168	0.199	0.075	3500.00	534.00	435.90	1.34	1.48	1.48	1.48	1.48	1.44
27	(Rasheed, 2016)	34.00	115	333	1200	1.20	1.83	0.083	0.336	0.075	3500.00	503.00	328.79	1.67	1.97	1.97	1.97	1.97	1.78
28	(Elsonbaty et al., 2018)	37.02	140	450	1900	1.25	4.30	0.269	0.269	0.186	3450.00	751.10	687.70	1.19	1.15	1.15	1.15	1.15	1.27
29	(Elsonbaty et al., 2018)	37.02	140	450	1900	1.25	4.30	0.269	0.269	0.243	3000.00	651.80	678.60	1.05	1.23	1.23	1.23	1.23	0.90
30	(Elsonbaty et al., 2018)	37.02	140	450	1900	1.75	4.30	0.269	0.269	0.186	3450.00	568.20	573.71	1.08	0.87	0.87	0.87	0.87	0.86
31	(Elsonbaty et al., 2018)	37.02	140	450	1900	1.75	4.30	0.269	0.269	0.243	3000.00	503.90	568.41	0.97	0.95	0.95	0.95	0.95	0.65
32	(Khudair & Atea, 2015)	45.89	175	300	1600	2.00	2.07	-	-	0.074	3500.00	490.00	484.60	1.11	2.38	2.38	2.38	2.38	1.75
33	(Khudair & Atea, 2015)	45.89	175	300	1600	2.00	2.07	-	-	0.074	3500.00	496.00	484.70	1.12	2.10	2.10	2.10	2.10	1.46
34	(Khudair & Atea, 2015)	45.89	175	300	1600	2.00	2.07	-	-	0.074	3500.00	500.00	484.60	1.13	2.43	2.43	2.43	2.43	1.79
35	(Khudair & Atea, 2015)	45.89	175	300	1600	2.00	2.07	-	-	0.074	3500.00	520.00	484.60	1.17	2.53	2.53	2.53	2.53	1.86
36	(Khudair & Atea, 2015)	45.89	175	300	1600	2.00	2.07	-	-	0.104	3500.00	504.00	491.80	1.12	2.15	2.15	2.15	2.15	1.59
37	(Khudair & Atea, 2015)	45.89	175	300	1600	2.00	2.07	-	-	0.104	3500.00	507.00	491.90	1.13	1.84	1.84	1.84	1.84	1.29
38	(Khudair & Atea, 2015)	45.89	175	300	1600	2.00	2.07	-	-	0.104	3500.00	512.00	491.80	1.14	2.18	2.18	2.18	2.18	1.62
39	(Khudair & Atea, 2015)	45.89	175	300	1600	2.00	2.07	-	-	0.104	3500.00	532.00	491.80	1.18	2.27	2.27	2.27	2.27	1.68

(continued)

Table 1. Continued.

No.	Ref.	f'_c (MPa)	b_w (mm)	h (mm)	L (mm)	a/d	ρ_s (%)	ρ_v (%)	ρ_h (%)	ρ_{FRP} (%)	f_{FRP} (MPa)	P_{uEXP} (kN)	P_{uSTM} (kN)	P_{uEXP} P_{uSTM}	$P_{u,ACI}$ (ACI Committee 440, 2008)	$P_{u,EXP}$ $P_{u,ACI}$ (ACI Antonopoulos, 2000)
40	(Khudair & Atea, 2015)	45.89	175	300	1600	2.00	2.07	-	-	0.092	3500.00	509.00	490.00	1.14	2.28	1.68
41	(Khudair & Atea, 2015)	45.89	175	300	1600	2.00	2.07	-	-	0.148	3500.00	498.00	494.80	1.10	1.79	1.17
42	(Asghari et al., 2014)	30.00	120	500	1500	0.95	1.49	0.157	0.157	0.293	4000.00	489.00	495.00	1.08	0.88	1.64
43	(Asghari et al., 2014)	30.00	120	500	1500	0.95	1.49	0.157	0.157	0.293	4000.00	528.00	506.00	1.14	0.78	1.68
44	(Asghari et al., 2014)	30.00	120	500	1500	0.95	1.49	0.157	0.157	0.667	3000.00	434.00	449.00	1.06	0.91	1.60
45	(Asghari et al., 2014)	30.00	120	500	1500	0.95	1.49	0.157	0.157	0.667	3000.00	460.00	459.00	1.10	0.81	1.67
46	(Islam et al., 2005)	37.80	120	800	2000	0.75	1.79	0.21	0.21	0.55	3480.00	1402.0	1215.00	1.26	0.94	2.13
47	(Islam et al., 2005)	37.80	120	800	2000	0.75	1.79	0.21	0.21	0.90	3050.00	1400.0	1214.00	1.26	0.96	2.13
48	(Javed et al., 2016)	41.80	152	381	1245	0.941	1.15	-	-	0.385	3800.00	640.00	780.00	0.90	1.05	3.44
49	(Javed et al., 2016)	41.80	152	381	1245	0.941	1.15	-	-	0.385	3800.00	615.00	766.00	0.88	1.31	3.66
50	(Al-Ahmed & Al-Jburi, 2016)	17.30	150	240	1100	1.547	1.63	0.38	-	0.10	3400.00	110.00	121.10	0.99	0.54	0.48
51	(Al-Ahmed & Al-Jburi, 2016)	17.30	150	240	1100	1.547	1.63	0.38	-	0.08	3400.00	107.80	120.00	0.98	0.55	0.47
52	(Al-Ahmed & Al-Jburi, 2016)	17.30	150	240	1100	1.547	1.63	0.38	-	0.067	3400.00	105.70	118.80	0.97	0.56	0.47
53	(Al-Ahmed & Al-Jburi, 2016)	17.30	150	240	1100	1.547	1.63	0.38	-	0.10	3400.00	107.10	120.70	0.97	0.52	0.41
54	(Al-Ahmed & Al-Jburi, 2016)	17.30	150	240	1100	1.547	1.63	0.38	-	0.08	3400.00	104.60	118.17	0.97	0.54	0.41
55	(Al-Ahmed & Al-Jburi, 2016)	17.30	150	240	1100	1.547	1.63	0.38	-	0.067	3400.00	102.30	116.61	0.96	0.54	0.41
										Average				1.160	1.36	1.49
										Standard deviation (SD)				0.180	0.56	0.67

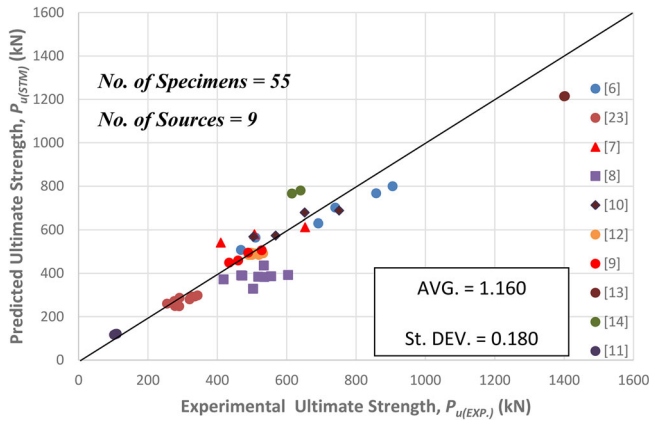


Figure 4. Comparison of the ultimate strength predictions using the proposed STM (Fathi, 2021) and the experimental results.

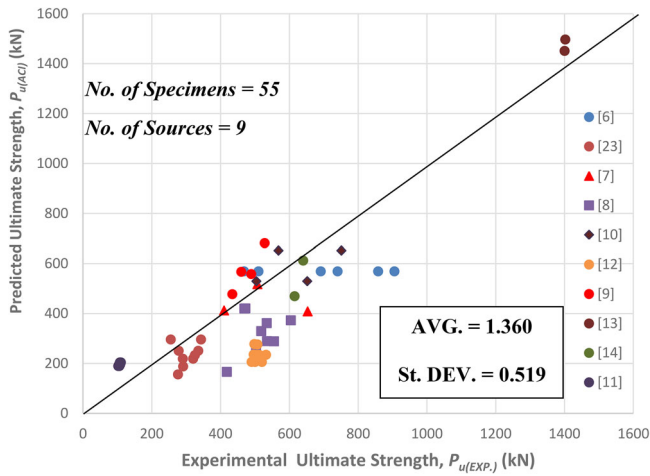


Figure 5. Comparison of the ultimate strength predictions using ACI code (ACI Committee 440, 2008) with the experimental results.

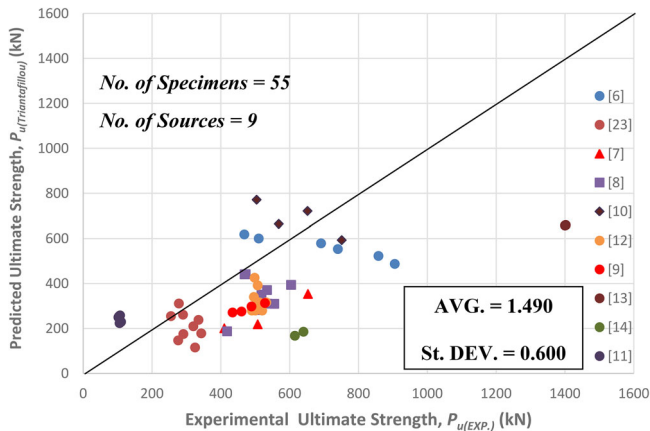


Figure 6. Comparison of the ultimate strength predictions using Triantafillou and Antonopoulos model (Triantafillou & Antonopoulos, 2000) with the experimental results.

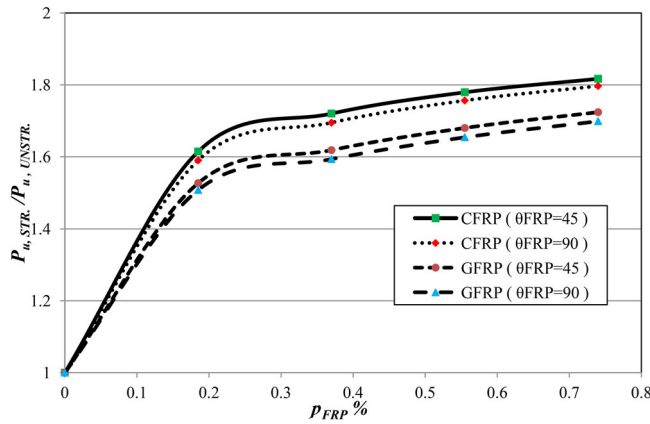


Figure 7. Effect of FRP ratio (p_{FRP}) and ($\theta_{w,FRP}$) on the ultimate strength predications.

The analysis procedure of the proposed (STM) for reinforced concrete deep beams strengthened with FRP materials can be easily presented by hand calculations or a spreadsheet. Fifty-five FRP-strengthened RC deep beams tested in references (Al-Ahmed & Al-Jburi, 2016; Al-Ghanem et al., 2017; Asghari et al., 2014; Elsonbaty et al., 2018; Hanoon, Jaafar, Hejazi, et al., 2017; Islam et al., 2005; Javed et al., 2016; Khudair & Atea, 2015; Panjehpour et al., 2014; Rasheed, 2016) have been analysed by the modified STM model (Fathi, 2021). The analysed deep beams having an overall depth ranged from (240 to 800 mm), the main longitudinal reinforcement ratios (ρ_s) ranging from (1.15% to 4.48%), having variables percentages of the vertical (ρ_v) and horizontal (ρ_h) stirrups ranged from (0.0% to 0.615%) and (0.0% to 0.757%), respectively, and shear span-to-depth ratio (a/d) ratio ranging from (0.75 to 2). The concrete cylindrical compressive strengths (f_c') ranged from (17.3 to 45.89 MPa). The tested deep beams strengthened with different FRP schemes having FRP shear strengthening ratios (ρ_{FRP}) ranged from (0.067% to 0.9%), the tensile strengths of FRP composite materials ranging from (2300 to 4900 MPa), having different strengthening configurations which include fully wrapped, U-shaped and two-opposite-sides FRP sheets or strips and having different fiber orientation angles with respect to the longitudinal axis of the deep beam. Detailed description for the studied parameters are tabulated in Table 1. The ultimate experimental load capacity ($P_{u(EXP)}$) and the theoretical ultimate capacity ($P_{u(STM)}$) using the proposed STM are shown in Figure 4. As presented in Figure 4; the proposed STM for reinforced concrete deep beams strengthened with FRP composite materials shows acceptable agreement in predicting the ultimate strengths. The overall average value of the ratio between the experimental capacity to the theoretical capacity of the proposed STM ($P_{u(EXP)}/P_{u(STM)}$) is of value 1.16 with a standard deviation of 0.18.

4. Comparative studies with design codes and pervious models

The relationships between the ultimate experimental capacity and theoretical capacity of the ACI Code 440 ($P_{u,ACI}$) (ACI Committee 440, 2008) and the previous model ($P_{u,tria}$) (Triantafillou & Antonopoulos, 2000) are displayed in Figures 5 and 6, respectively. As shown in Figures 5 and 6; for the ACI code (ACI Committee 440, 2008) the overall average value of the ratio between the experimental capacity to the predicted capacity ($P_{u,EXP}/P_{u,ACI}$) is of value 1.36 and a standard deviation of 0.56. The overall average value of the ratio between the experimental capacity to the predicted capacity ($P_{u,EXP}/P_{u,tria}$) is of value 1.49 and a standard deviation of 0.67 for Triantafillou and Antonopoulos model (Triantafillou & Antonopoulos, 2000). As observed from the obtained results; the ACI Code (ACI Committee 440, 2008) and the Triantafillou and Antonopoulos model (Triantafillou & Antonopoulos, 2000) are more conservative results than the proposed STM. This can be attributed to the fact that the ACI Code (ACI Committee 440, 2008) and the Triantafillou and Antonopoulos model (Triantafillou & Antonopoulos, 2000) have considered the concrete softening effect in the calculation of shear strength in an approximate and simplified manner using constant reduction factors.

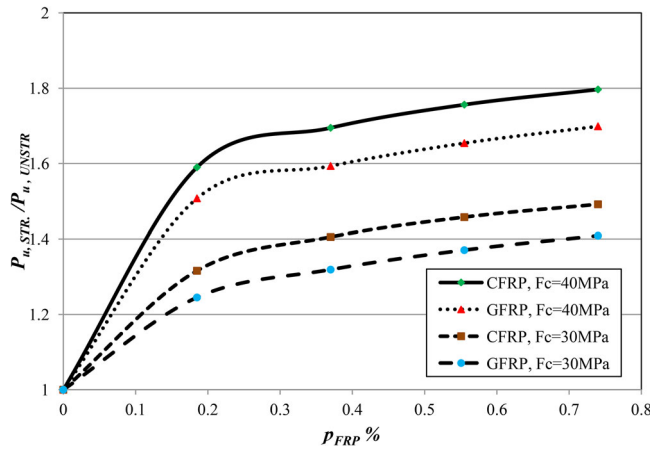


Figure 8. Effect of FRP ratio (p_{FRP}) and (f_c) on the ultimate strength predications.

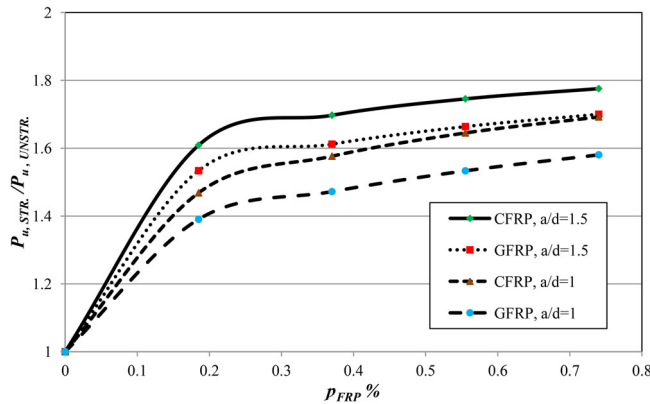


Figure 9. Effect of FRP ratio (p_{FRP}) and (a/d) on ultimate strength predications.

5. FRP effectiveness studies for shear strengthening of deep beams

To verify the effectiveness of the modified STM on the shear behaviour of FRP-strengthened deep beams, a parametric study is performed using different material and geometry parameters. Using the modified STM, the enhancement of the shear strength resulted from the FRP strengthening of deep beams was calculated for all considered cases with different parameters. Then, the effect of different parameters on the ratio between the ultimate strength for FRP-strengthened deep beams ($P_{u,STR}$) and the ultimate strength for RC deep beams without strengthening ($P_{u,UNSTR}$) was recorded. The following material and geometry parameters are considered in this study:

1. Parameters of FRP strengthening materials, as shown in Figure 7
2. Concrete compressive strength (f_c) parameter as shown in Figure 8
3. Geometry parameter or (a/d) ratio parameter as shown in Figure 9

The effect of FRP ratio (p_{FRP}), FRP material type (CFRP or GFRP) and inclination angle on the ultimate strength of RC deep beams is illustrated in Figure 7. From the figure, it can be concluded that the ultimate strength of RC deep beams strengthened with FRP materials is improved by increasing FRP ratio (p_{FRP}). Higher increase percentages for the ultimate strength are predicted for CFRP strengthening which has higher tensile strength, than GFRP strengthening. For fiber orientation angle with a value of 45 degrees to the longitudinal axis of the deep beam, the ultimate strength shows better enhancement when compared with deep beam having fiber orientation angle with a value of 90 degrees. Keeping the

fiber orientation angle as 90 degrees, the increase of (p_{FRP}) from 0.0 to 0.75% enhances ($P_{u,STR}$) by 69% for GFRP-strengthened deep beam, and by 79% for CFRP-strengthened deep beams. Keeping CFRP ratio as 0.37%, ($P_{u,STR}$) showed improvement by 69% when using fiber orientation angle is 90 degrees, and by 72% when using fiber orientation angle of 45 degree to the longitudinal axis of the deep beam.

Figure 8 shows the effect of FRP ratio (p_{FRP}), FRP material type (CFRP or GFRP) and concrete strength (f_c') on the ultimate strength of RC deep beams. As presented in Figure 8, the ultimate strength of RC deep beams strengthened with FRP materials is improved by increasing the concrete compressive strength (f_c'). Keeping CFRP ratio as 0.37%, ($P_{u,STR}$) improves the ultimate strength of deep beam by 40% with concrete compressive strength of 30 MPa, and by 69% with concrete compressive strength of 40 MPa.

The effect of shear span to depth ratio on the predicted shear capacities of FRP-strengthened deep beams is shown in Figure 9. Generally, the ultimate strengths of un-strengthened and FRP-strengthened RC deep beams are inversely proportional to shear span-to-depth ratio (a/d). However, the ratio ($P_{u,STR}/P_{u,UNSTR}$) is directly proportional to (a/d) ratio as displayed in Figure 9. Keeping CFRP ratio as 0.37%, the ratio ($P_{u,STR}/P_{u,UNSTR}$) has a value of 1.57 for (a/d) ratio equals 1.0 and a value of 1.69 for (a/d) ratio equals 1.50.

6. Conclusions

From the predictions and FRP effectiveness studies of the proposed STM, the following points are concluded:

1. Applying the modified STM to predict the shear capacity of 55 specimens in the literature showed that the modified STM is performing well in estimating the ultimate loads of reinforced concrete deep beams strengthened with FRP composites. The overall average value of the ratio between the experimental capacity to the theoretical capacity of the proposed STM ($P_{u(EXP)}/P_{u(STM)}$) is of value 1.16 with a standard deviation of 0.18.
2. The comparison between the experimental results and analytical results from the ACI Code 440 (ACI Committee 440, 2008) and the Triantafillou and Antonopoulos model (Triantafillou & Antonopoulos, 2000) indicates that the available codes are more conservative than the modified STM. The overall average ratio between the experimental load and the predicted capacity is of values 1.36 and 1.49 with standard deviations of 0.56 and 0.67 for ACI Code (ACI Committee 440, 2008) and Triantafillou model (Triantafillou & Antonopoulos, 2000), respectively.
3. The ultimate strength of RC deep beams strengthened with FRP materials is improved by increasing FRP ratio (p_{FRP}). Higher increase percentages are predicted for CFRP which has higher tensile strength than GFRP, and for fiber orientation angle equals 45 degree to the longitudinal axis of the deep beam. Considering the direction of fiber is vertical, the increase of (p_{FRP}) from 0.0 to 0.75% enhances ($P_{u,STR}$) by 69% for GFRP-strengthened deep beam, and by 79% for CFRP-strengthened deep beams. Keeping CFRP ratio as 0.37%, ($P_{u,STR}$) is improved by 69% when fiber direction is vertical and by 72% when using fiber orientation angle equals 45 degree.
4. The ultimate strength of RC deep beams strengthened with FRP materials is improved by increasing the concrete compressive strength (f_c'). Keeping CFRP ratio as 0.37%, ($P_{u,STR}$) improves by 40% with concrete compressive strength of 30 MPa, and by 69% with concrete compressive strength of 40 MPa.
5. Generally, the ultimate strengths of un-strengthened and FRP-strengthened RC deep beams are inversely proportional to shear span-to-depth ratio (a/d) but the ratio ($P_{u,STR}/P_{u,UNSTR}$) is directly proportional to (a/d) ratio. Keeping CFRP ratio as 0.37%, the ratio ($P_{u,STR}/P_{u,UNSTR}$) has a value of 1.57 for (a/d) ratio equals 1.0 and a value of 1.69 for (a/d) ratio equals 1.5.

Nomenclature

a/d	the shear span-to-depth ratio
A_c	the cross- sectional area of the deep beam
A_{FRP}	the total area of the FRP material
A_s	the total area of the longitudinal steel reinforcement

A_{sh}	the total area of the horizontal web steel reinforcement within the distance of the shear span
A_{str}	the cross- sectional area of the diagonal strut
A_{sv}	the total area of the vertical web steel reinforcement within the distance of the shear span
A_w	the total area of the web steel reinforcement
b_w	the width of the deep beam
f_c'	the concrete cylindrical compressive strength
F_c	The compressive force applied through the inclined strut
$F_{f,FRP}$	the ultimate strength of the FRP material
ft	the tensile strength contribution of concrete
f_y	the yield strength of the longitudinal steel reinforcement
f_{yh}	the yield strength of the horizontal web steel reinforcement
f_{yv}	the yield strength of the vertical web steel reinforcement
f_{yw}	the yield strength of the web steel reinforcement
f_1	the transverse tensile stress
f_2	the compressive stress
h	the overall depth of the deep beam
K_1 and K_2	the stress distribution factors
L	the span of the deep beam
l_a	the depth of the bottom nodal zone of the inclined strut
l_b	the width of the support-bearing plate
l_c	the depth of the top nodal zone of the inclined strut
n_f	the number of the FRP material layers
$P_{u(EXP)}$	the experimental capacity of the proposed STM
$P_{u(STM)}$	the theoretical capacity of the proposed STM
T	the tensile force applied through the horizontal tie
V_n	the nominal shear capacity
Z_s	the lever arm connected between the longitudinal reinforcement and the center of the upper node of the diagonal strut
ρ_{FRP}	the FRP ratio
ρ_h	the horizontal shear reinforcement ratio
ρ_s	the main longitudinal reinforcement ratio
ρ_v	the vertical shear reinforcement ratio
θ_s	the angle of inclination of the inclined strut
θ_w	the angle of inclination of the inclined web reinforcement with the longitudinal axis
$\theta_{w,FRP}$	the orientation angle of the FRP material with respect to the longitudinal axis of the deep beam

Acknowledgement

Not Applicable

Conflict of interest

The authors declare that they have no conflict of interest.

Declaration of competing interest

The authors declare that they have no known competing financial interests or personal relationships that could have appeared to influence the work reported in this article. The authors acknowledge their contribution in this study.

Consent to publication

The authors declare their consent for publication.

Data availability

The authors declare that all the data are available if required.

References

- ACI Committee 318. (2014). Building Code Requirements for Structural Concrete (ACI 318M-14) and Commentary (ACI 318RM-14). American Concrete Institute.
- ACI Committee 440. (2008). *State-of-the-art report on externally bonded FRP systems for strengthening concrete structures*. American Concrete Institute.
- Al-Ahmed, A. H. A., & Al-Jburi, M. H. M. (2016 August). Behavior of reinforced concrete deep beams strengthened with carbon fiber reinforced polymer strips. *Journal of Engineering*, 22(8), 37–53.
- Al-Ghanem, H., Al-Asi, A., Abdel-Jaber, M., & Alqam, M. (2017). Shear strengthening of reinforced concrete deep beams using carbon fiber reinforced polymers. *Modern Applied Science*, 11(10), 110. <https://doi.org/10.5539/mas.v11n10p110>
- Asghari, A. A., Tabrizian, Z., Beygi, M. H., Amiri, G. G., & Navayineya, B. (2014). An experimental study on shear strengthening of RC lightweight deep beams using CFRP. *Journal of Rehabilitation in Civil Engineering*, 2(2), 9–19.
- Bungale, S., & Taranath, A. (2012). *Reinforced concrete design of tall buildings handbook* (pp. 85–90). Concrete Reinforcing Steel Institute.
- CEB-FIP. (1993). CEB-FIP. Model Code 1990: Design Code. Comite Euro-International du Beton.
- CSA-A23.3. (1994). Design of concrete structures (A23.3-94). Canadian Standards Association.
- El Maaddawy, T., & Sherif, S. (2009). FRP composites for shear strengthening of reinforced concrete deep beams with openings. *Composite Structures*, 89(1), 60–69. <https://doi.org/10.1016/j.compstruct.2008.06.022>
- Elsonbaty, M. M., Montaser, W. M., & Zaher, A. H. (2020 October). Strengthening and repairing of RC deep beams using CFRP, GFRP. *International Journal of Civil Engineering and Technology*, 40(4), 64–85.
- Fathi, M. G. (2021). *Shear assessment of FRP-strengthened reinforced concrete deep beams* [MSc thesis]. Faculty of Engineering.
- Foster, S. J. (1992). The structural behavior of reinforced concrete deep beams. University of New South Wales.
- Hanoon, A., Jaafar, M. S., Al Zaidee, S., Hejazi, F., & Aziz, A. (2017). Effectiveness factor of the strut-and-tie model for reinforced concrete deep beams strengthened with CFRP sheet. *Journal of Building Engineering*, 12, 8–16. ELSEVIER <https://doi.org/10.1016/j.jobbe.2017.05.001>
- Hanoon, A. N., Jaafar, M. S., Hejazi, F., A., & Aziz, F. N. A. (2017). Strut-and-tie model for externally bonded CFRP-strengthened reinforced concrete deep beams based on particle swarm optimization algorithm: CFRP debonding and rupture. *Construction and Building Materials*, 147, 428–447.
- Hawileh, R. A., El-Maaddawy, T. A., & Naser, M. Z. (2012). Nonlinear finite element modeling of concrete deep beams with openings strengthened with externally-bonded composites. *Materials & Design*, 42, 378–387. <https://doi.org/10.1016/j.matdes.2012.06.004>
- Hawileh, R. A., Nawaz, W., Abdalla, J. A., & Saqan, E. I. (2015). Effect of flexural CFRP sheets on shear resistance of reinforced concrete beams. *Composite Structures*, 122, 468–476. <https://doi.org/10.1016/j.compstruct.2014.12.010>
- Islam, M. R., Mansur, M. A., & Maalej, M. (2005). Shear strengthening of RC deep beams using externally bonded FRP systems. *Cement and Concrete Composites*, 27(3), 413–420. <https://doi.org/10.1016/j.cemconcomp.2004.04.002>
- Javed, M. A., Irfan, M., Khalid, S., Chen, Y., & Ahmed, S. (2016). An experimental study on the shear strengthening of reinforced concrete deep beams with carbon fiber reinforced polymers. *KSCE Journal of Civil Engineering*, 20(7), 2802–2810. <https://doi.org/10.1007/s12205-016-0739-3>
- Karayannis, C. G., & Goliias, E. (2018). Full scale tests of RC joints with minor to moderate seismic damage repaired using C-FRP sheets. *Earthquakes and Structures*, 15(6), 617–627.
- Khudair, J. A., & Atea, R. S. (2015). Shear behavior of self-compacting concrete deep beams strengthened with carbon fiber reinforced polymer sheets. *International Journal of Engineering Research & Technology*, 4(02), 187–191.
- McCormac, J. C., & Brown, R. (2014). Design of reinforced concrete handbook (9th ed., pp. 675–682). ACI.

- Naser, M. Z., Hawileh, R. A., & Abdalla, J. A. (2019). State-of-the-art review on the use of fiber-reinforced polymer composites in civil constructions. *Engineering Structures*, 198, 109542. <https://doi.org/10.1016/j.engstruct.2019.109542>
- Nawaz, W., Hawileh, R. A., Saqan, E. I., & Abdalla, J. A. (2016). Effect of longitudinal carbon fiber-reinforced polymer plates on shear strength of reinforced concrete beams. *ACI Structural Journal*, 113(3), 577. <https://doi.org/10.14359/51688475>
- Panjehpour, M., Ali, A., Voo, Y., & Aznieta, F. (2014). Modification of strut effectiveness factor for reinforced concrete deep beams strengthened with CFRP laminates. *Materiales de Construccion*, 64(314), 1–8.
- Rasheed, M. M. (2016). Retrofit of reinforced concrete deep beams with different shear reinforcement by using CFRP. *Civil and Environment Research*, 8(5), 6–14.
- Tan, K., Tong, K., & Tang, C. (2001). Direct strut-and-tie model for prestressed deep beams. *Journal of Structural Engineering*, 127(9), 1076–1084. [https://doi.org/10.1061/\(ASCE\)0733-9445\(2001\)127:9\(1076\)](https://doi.org/10.1061/(ASCE)0733-9445(2001)127:9(1076))
- Tanapornraweekit, G., Haritos, N., & Mendis, P. (2011). Behavior of FRP-RC slabs under multiple independent air blasts. *Journal of Performance of Constructed Facilities*, 25(5), 433–440. [https://doi.org/10.1061/\(ASCE\)CF.1943-5509.0000191](https://doi.org/10.1061/(ASCE)CF.1943-5509.0000191)
- Tang, C., & Tan, K. (2004). Interactive mechanical model for shear strength of deep beams. *Journal of Structural Engineering*, 130(10), 1534–1544. [https://doi.org/10.1061/\(ASCE\)0733-9445\(2004\)130:10\(1534\)](https://doi.org/10.1061/(ASCE)0733-9445(2004)130:10(1534))
- Tong, K. (1997). Strut-and-tie approach to shear strength prediction of deep beams [MEng thesis]. Nanyang Technological University.
- Triantafillou, T. C., & Antonopoulos, C. P. (2000). Design of concrete flexural members strengthened in shear with FRP. *Journal of Composites for Construction*, 4(4), 198–205. [https://doi.org/10.1061/\(ASCE\)1090-0268\(2000\)4:4\(198\)](https://doi.org/10.1061/(ASCE)1090-0268(2000)4:4(198))
- Ugural, A. C., & Fenster, S. K. (2003). *Advanced strength and applied elasticity*. Pearson Education.
- Vecchio, F. J., & Collins, M. P. (1986). *The modified compression-field theory for reinforced concrete elements subjected to shear*. ACI.
- Zeng, L. H., & Tan, K. H. (1999). *Normal-strength reinforced concrete deep beams: A direct approach to design*. N.T.U. National.